Metallointercalator $[Ru(dppz)_2(PIP)]^{2+}$ renders BRCA wild-type triple-negative breast cancer cells hypersensitive to PARP inhibition

Nur Aininie Yusoh,[†] Sze Wei Leong,[‡] Suet Lin Chia, [‡,¶] Siti Norain Harun,[†] Mohd Basyaruddin Abdul Rahman, [†,‖] Katherine A. Vallis,[⊥] Martin R. Gill,[§]* and Haslina Ahmad[†,‖]*

[†]Department of Chemistry, Faculty of Science, Universiti Putra Malaysia, 43400 UPM Serdang, Selangor, Malaysia
[‡]Department of Microbiology, Faculty of Biotechnology and Biomolecular Sciences, Universiti Putra Malaysia, 43400 UPM Serdang, Selangor, Malaysia
[¶]Institute of Bioscience, Universiti Putra Malaysia, 43400 UPM, Serdang, Selangor, Malaysia
[‖]Integrated Chemical Biophysics Research Centre, Faculty Science, Universiti Putra Malaysia, 43400 UPM Serdang, Selangor, Malaysia.
[⊥]Oxford Institute for Radiation Oncology, Department of Oncology, University of Oxford, Oxford, UK.
[§]Department of Chemistry, College of Science, Swansea University, Swansea, Wales, UK.

Abstract

There is a need to improve and extend the use of clinically-approved poly(ADP-ribose) polymerase (PARP) inhibitors (PARPi), including for BRCA wild-type triple-negative breast cancer (TNBC). The demonstration that ruthenium(II) polypyridyl complex (RPC) metallo-intercalators can rapidly stall DNA replication fork progression provides the rationale for their combination alongside DNA damage response (DDR) inhibitors to achieve synergism in cancer cells. The aim of the present study was to evaluate use of the multi-intercalator $[Ru(dppz)_2(PIP)]^{2+}$ (dppz = dipyrido[3,2-a:2′,3′-c]phenazine, PIP = (2-(phenyl)imidazo[4,5-f][1,10]phenanthroline, Ru-PIP) alongside the PARP inhibitors (PARPi) olaparib and NU1025. Cell proliferation and clonogenic survival assays indicated a synergistic relationship between Ru-PIP and olaparib in MDA-MB-231 TNBC and MCF7 human breast cancer cells. Strikingly, low dose Ru-PIP renders both cell lines hypersensitive to olaparib, with a 300-fold increase in olaparib potency in TNBC; the largest non-genetic PARPi enhancement effect described to date. Negligible impact on the viability of normal human fibroblasts was observed for any combination tested. Increased levels of DNA double-strand

break (DSB) damage and olaparib abrogation of Ru-PIP activated pChk1 signalling is consistent with PARPi-facilitated collapse of Ru-PIP-associated stalled replication forks. This results in enhanced G2/M cell-cycle arrest, apoptosis and decreased cell motility for the combination treatment compared to single-agent conditions. This work establishes that an RPC metallo-intercalator can be combined with PARPi for potent synergy in BRCA-proficient breast cancer cells, including TNBC.

Introduction

Breast cancer remains a leading cause of death in women, and approximately 10-24% of all invasive breast cancers are triple negative (TNBC) or basal-like breast cancers (BLBC).[1] TNBC cannot be treated with endocrine therapy or targeted therapeutics such as the anti-HER2 (human epidermal growth factor receptor 2) agent trastuzumab.[2] TNBC can respond to chemotherapy, however, relapse is frequent.[3] As a result, this subgroup of breast cancer accounts for a disproportionately high rate of mortality and new approaches are required to improve upon the limited therapeutic options available for TNBC at present.[4]

A leading class of candidates for TNBC treatment are small molecule inhibitors of poly(ADP-ribose) polymerase (PARP) enzymes.[2] PARPs are DNA repair proteins that play a key role in the repair of single-strand breaks (SSB), preventing the generation of cytotoxic double-strand breaks (DSBs).[5] As cells that contain BRCA1/2 gene mutations possess an inherent deficiency in the homologous recombination (HR) repair of DSBs, this results in synthetic lethality between BRCA1/2 deficiency and PARP inhibition.[6,7] Accordingly, PARP inhibitors (PARPi) have been developed as single-agent treatments for BRCA1/2-deficient breast, ovarian and prostate cancers.[8] The PARPi olaparib (Lynparza®) recently passed phase III clinical trials for metastatic BRCA1/2-deficient breast cancer, including TNBC subtypes, and is now FDA-approved.[9] However, response to PARPi treatment is often heterogenous[10] and a relatively low frequency of cancers are BRCA-deficient (thought to be <10% of TNBC patients, although inherent BRCA mutations are higher in certain ethnic groups[11]). Due to this, there is an identifiable need to improve the efficacy of clinically-approved PARPi and extend their application to BRCA wild-type cancers.[12] As such, studies have examined PARPi alongside traditional DNA-damaging chemotherapeutics to identify synergistic combinations. For example, recent studies have shown olaparib to have a synergistic

relationship in combination with cisplatin,[13] carboplatin,[14] or doxorubicin.[15] Moreover, clinical trials have examined olaparib alongside platinum agents for both breast and cervical cancers.[16–18] However, significant off-target toxicity from some of these drug combinations was noted due to overlapping toxicity profiles, particularly in bone marrow.[19] Other candidates shown to sensitize BRCA wild-type cancer cells to PARPi in pre-clinical studies include other inhibitors of DNA damage response (DDR) proteins such as WEE1,[20] ATR (Ataxia telangiectasia and Rad3 related)[21] or DNA demethylating agents.[22] However, all these agents generate substantial DSB damage. As PARPi likewise generates DSBs to exert their cytotoxic effects, this mechanistic overlap may contribute to unfavourable toxicity and myelosuppression observed in clinical trials.[23] Towards this end, new synergistic PARPi chemical combination strategies for use in BRCA wild-type cancers remain highly desirable.[24]

In addition to the role of PARPs in SSB repair, PARP1 and PARP2 also play a crucial role in the stabilization of stalled replication forks and function to promote fork restart.[25–27] It follows that PARPi alongside replication inhibition can facilitate fork collapse, resulting in DSB formation and synthetic lethality.[27] As a novel chemical combination strategy for PARPi, ruthenium(II) polypyridyl complexes (RPCs) that bind DNA by metallo-intercalation (reviewed in reference 28) have been shown to inhibit DNA replication in cancer cells, activating DNA damage response (DDR) signaling and preventing cell proliferation by interfering with cell-cycle progression.[29,30] Of particular interest, the multi-intercalator $[Ru(dppz)_2(PIP)]^{2+}$ (dppz = dipyrido[3,2-a:2′,3′-c]phenazine, PIP = (2-(phenyl)imidazo[4,5-f][1,10]phenanthroline, referred to as Ru-PIP hereafter, Figure 1A) generates high levels of stalled DNA replication forks *without* an associated DSB response or triggering apoptosis, indicating stalled forks do not collapse.[29] With this in mind, we hypothesized that Ru-PIP would be a strong candidate to achieve synergy with PARPi. In this study, we explore Ru-PIP in combination with the FDA-approved PARPi olaparib (OLAP, Figure 1A) in BRCA wild-type human breast cancer cells, including TNBC, and explore the mechanistic basis for this novel therapeutic combination strategy.

Results and Discussion

Single-agent activities. First, the anti-proliferative potency of Ru-PIP and OLAP (IC_{50} = 5 nM and 1 nM for inhibiting purified PARP1 and PARP2 enzymes respectively)[12] as single-

agents was examined. The first generation PARP inhibitor NU1025 (PARP1 half maximal enzyme inhibitory concentration, IC_{50} = 400 nM)[31] was included for comparative purposes (Figure 1A). MDA-MB-231 TNBC and MCF7 breast cancer cells, both of which are BRCA wild-type,[32] were treated with a concentration gradient of the compounds and the resultant impact on cell proliferation determined by MTT assay. These experiments indicated that Ru-PIP caused a dose- and time-dependent decrease in cell viability of both breast cancer cell lines, with greater potency towards MCF7 cells compared to MDA-MB-231 TNBC (72 h half-inhibitory EC_{50} concentrations of 7 and 29 μM, respectively, Figure 1B and Supplementary Table 1). Each PARPi showed low activity, with all EC_{50} values > 60 μM, as expected given that BRCA wild-type cells are not sensitive to PARPi in isolation. Treatment of the non-malignant normal human dermal fibroblasts (NHDF) cells showed minimal inhibitory effect for any compound, with EC_{50} values >100 μM (Figure 1B, Supplementary Table 1).

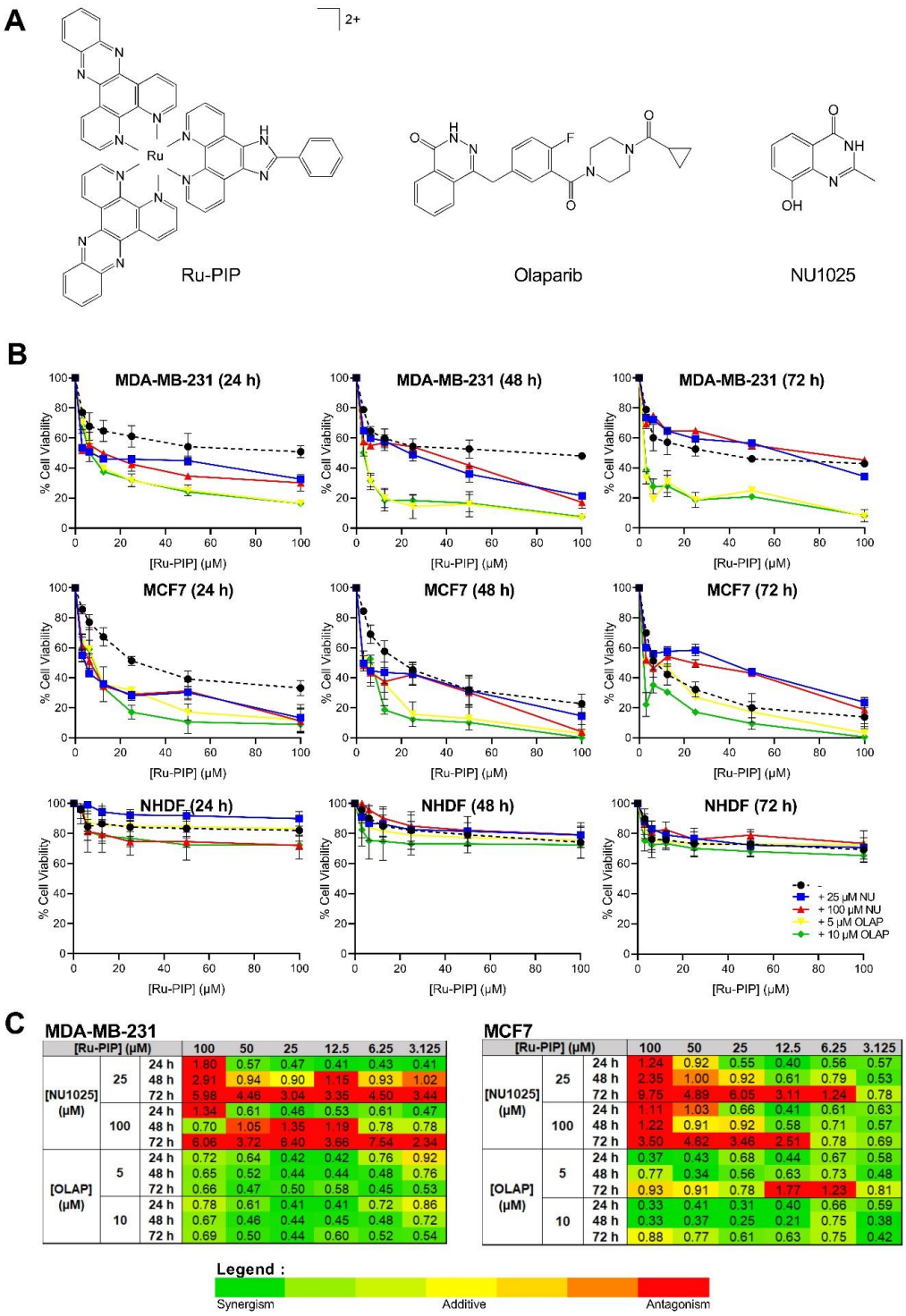

Figure 1. PARPi synergizes with Ru-PIP. (A) Chemical structures of $[Ru(dppz)_2(PIP)]^{2+}$ (Ru-PIP) and the PARP inhibitors olaparib and NU1025. (B) Cell viability of MDA-MB-231 TNBC, MCF7 breast cancer and normal NHDF fibroblast cells upon treatment with various Ru-PIP-PARPi combinations for 24, 48 and 72 h, as determined by MTT assay (described within the Supplementary Methods section). Non-cytotoxic doses of OLAP (5 or 10 μM) or NU1025 (25 or 100 μM) were used in the combination treatments. Data is presented as mean

+/- SD for three independent experiments. (C) Combination indices (CI) for Ru-PIP with OLAP or NU1025 in MCF7 or MDA-MB-231 cells for 24, 48 or 72 h treatment. CI values were calculated and a heat map generated as described within the Methods section.

Olaparib synergizes with Ru-PIP in breast cancer cells. To assess Ru-PIP in combination with PARPi, MDA-MB-231 or MCF7 cells were exposed to sub-cytotoxic doses of OLAP and NU1025 alongside a concentration gradient of Ru-PIP. The resultant impact on cell viability was determined by MTT assay. In this manner we can show Ru-PIP and OLAP combination treatment was able to significantly decrease breast cancer cell viability compared to single-agent conditions (Figure 1B). Median-effect analysis based on Chou and Talalay[33] were performed and combination indices (CI) derived. Applying this method, the vast majority of the Ru-PIP/OLAP conditions tested were deemed synergistic (Figure 1C). Ru-PIP/NU1025 showcased a range of combination indices, ranging from synergistic to antagonistic. The lack of conclusive synergy between Ru-PIP and NU1025 is likely due to the reduced potency of NU1025 for PARP inhibition compared to olaparib. Sequential treatment experiments of Ru-PIP and OLAP established co-administration to be the most effective for synergy in MCF7 cells with no obvious sequential and co-administration dependence in MDA-MB-231 cells (Supplementary Figure 1). Negligible effects of any combination on non-malignant NHDF cells was observed, with cell viabilities > 70% compared to mock-treated at 72 h incubation time (Figure 1B and Supplementary Table 1).

Ru-PIP renders breast cancer cells hypersensitive to olaparib. Next, the impact of Ru-PIP and PARPi on long-term cell survival was assessed by clonogenic survival assay. Single-agent Ru-PIP was not found to impact cell survival at 24 h incubation and low impact of NU1025 was observed (survival fractions, S.F. > 80%, Figure 2A). While OLAP had a modest impact on survival of MDA-MB-231 cells, an almost total loss of clonogenic potential in both cell lines were observed upon co-treatment with Ru-PIP/OLAP (Figure 2A). Ru-PIP and NU1025 in combination also induced a more potent impact on cell survival together than as single-agents, although a longer incubation time of 48 h was required to see this effect in MCF7 cells (Figure 2A). The greater synergy observed between Ru-PIP and OLAP in the clonogenic studies are consistent with the MTT results and may be rationalised by the greater PARPi properties of olaparib compared to NU1025.

To investigate whether Ru-PIP altered cell sensitivity to PARPi, cells were treated with concentration gradients of OLAP with or without Ru-PIP. As shown in Figure 2B, MDA-MB-231 cells treated with Ru-PIP were rendered hypersensitive to OLAP, where a >300-fold increase in OLAP potency was seen (OLAP EC_{50} values of 0.06 μM and 23.4 μM in the presence and absence of Ru-PIP, respectively). Similar results albeit at a reduced magnitude were found in MCF7 cells, with a 60-fold increase in OLAP potency observed due to addition of Ru-PIP (OLAP EC_{50} values of 0.08 μM and 4.8 μM for MCF7 in the presence and absence of Ru-PIP, respectively). Single-agent Ru-PIP had low impact on colony formation (S.F.s > 80%). These data indicate a strong synergistic relationship between Ru-PIP and PARPi in impacting cell survival of these two breast cancer cell lines and also reveal the unanticipated outcome that Ru-PIP renders these breast cancer cells hypersensitive to OLAP. To the best of our knowledge, the 300-fold increase of OLAP efficacy generated by co-treatment with Ru-PIP in BRCA wild-type TNBC cells is the greatest enhancement of OLAP by a small molecule that has been described to date.

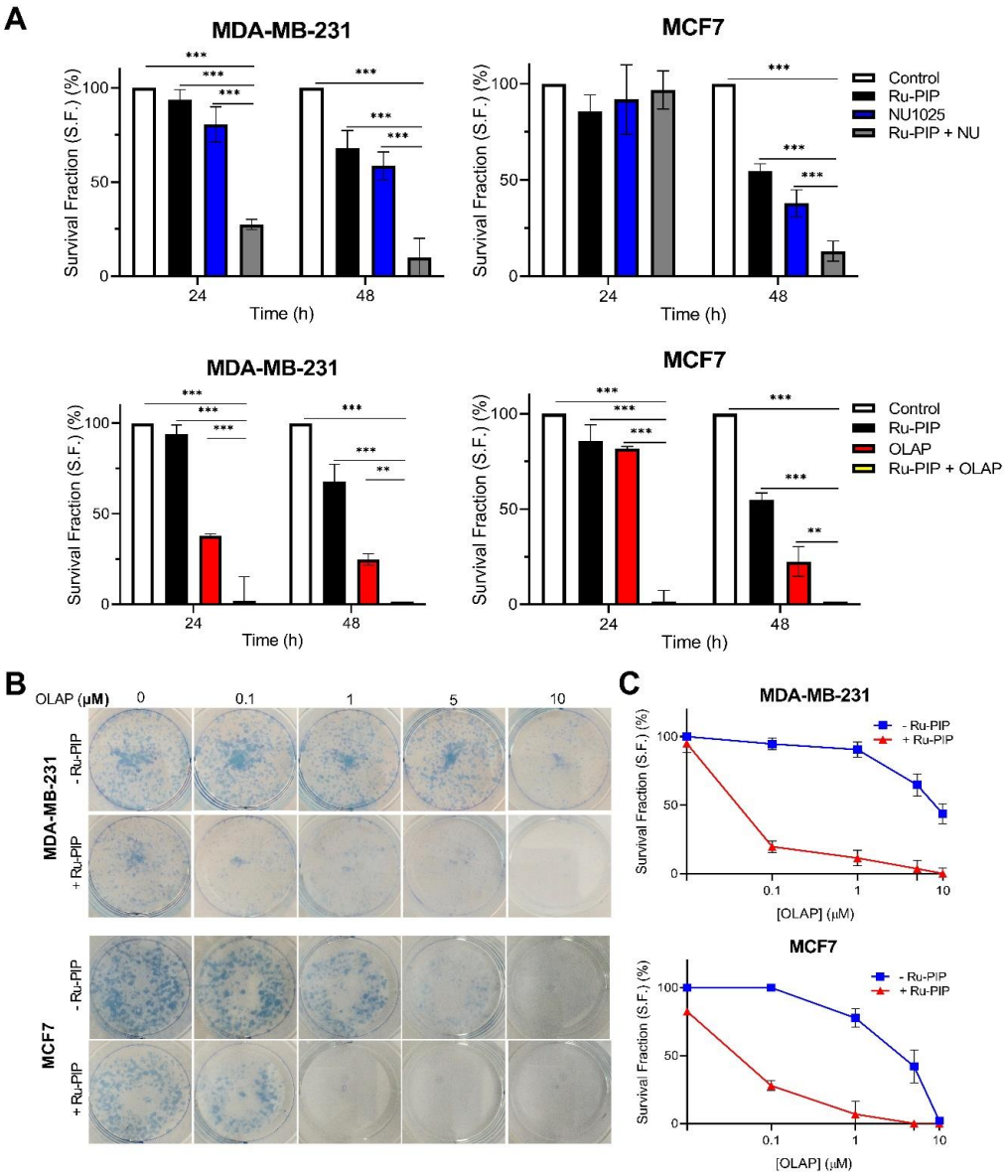

Figure 2. Ru-PIP renders breast cancer cells hypersensitive to olaparib. (A) Clonogenic survival assays of MDA-MB-231 or MCF7 cells exposed to Ru-PIP (25 μM), NU1025 (25 μM), OLAP (5 μM) or both (24 h treatment). (B) Clonogenic assays of MDA-MB-231 or MCF7 cells treated with a concentration gradient of OLAP in the absence or presence of Ru-PIP (25 μM). 24 h treatment. (C) Quantification of survival fraction of cells treated as in (B). Mean +/- SD for three independent experiments. *P < 0.05, **P < 0.01, ***P < 0.001 by ANOVA.

Ru-PIP/olaparib increases G2/M arrest and apoptotic cell death. The cell cycle response of MDA-MB-231 and MCF7 cells upon treatment with Ru-PIP and/or OLAP for 24 h and cell cycle progression was analyzed by flow cytometry. Ru-PIP as a single agent caused a

small increase in G1/early S phase populations in both cell lines in comparison to control (Figure 3A). OLAP as a single-agent was able to arrest the cells in G2/M phase even at a sub-lethal dose, while the Ru-PIP-OLAP combination treatment further increased cell cycle arrest at G2/M phase (Figure 3A). Meanwhile, treatment with the Ru-PIP/NU1025 combination did not significantly alter cell-cycle distribution in MDA-MB-231 cells and caused only a slight increase in G2/M arrest in MCF7 cells in comparison to control (Supplementary Figure 2). We next examined apoptosis by using Annexin V-FITC/PI co-staining. MDA-MB-231 and MCF7 cells were exposed to Ru-PIP and/or OLAP for 24 and 48 h. Both Ru-PIP and OLAP as single-agents induced low levels of apoptosis in breast cancer cells in comparison to control, however, the Ru-PIP/OLAP combination resulted in a substantially higher percentage of apoptotic cell death than either single-agent treatment (Figures 3B). Additionally, an increase in Trypan blue-positive cells was observed upon Ru-PIP/OLAP combined treatment versus single-agent conditions, confirming that Ru-PIP/OLAP combinations caused an increase in cell death in comparison to single agents (Supplementary Figure 3). These data are consistent with the synergistic effect observed in previous experiments and indicates that the combination is cytotoxic rather than cytostatic.

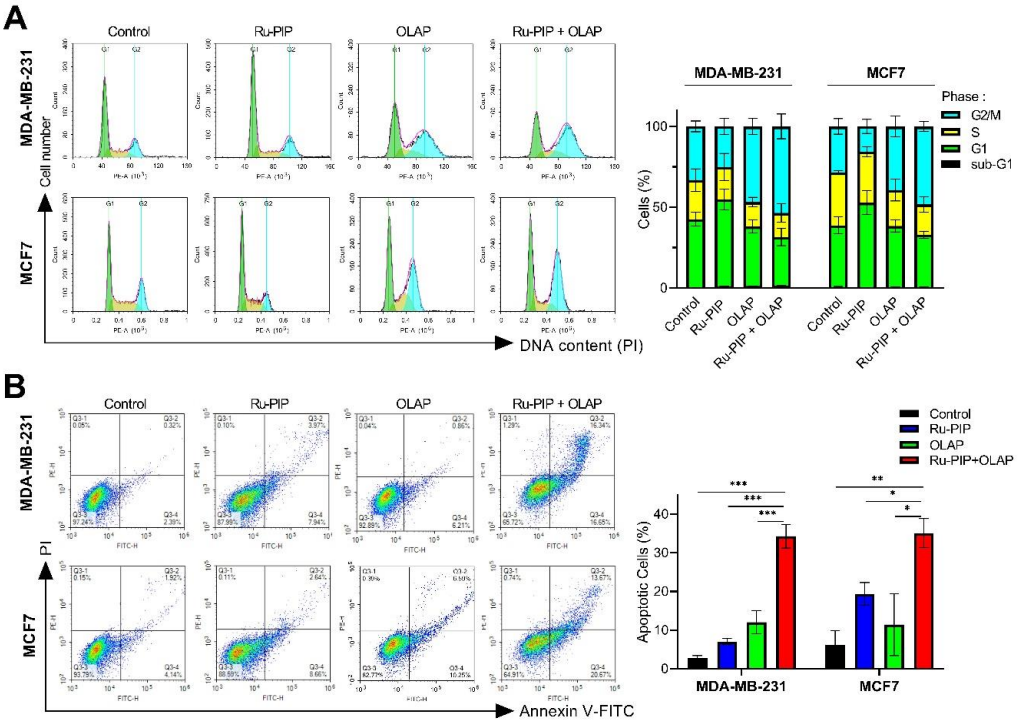

Figure 3. Ru-PIP/olaparib combination results in G2/M arrest and enhanced apoptosis. (A) Cell-cycle distributions of MDA-MB-231 or MCF7 cells incubated with Ru-PIP (25 μM), OLAP (5 μM), or both, for 24 h. DNA content was quantified using propidium iodide (PI)

and cell-cycle phase analyzed by flow cytometry, as described in the Materials and Methods. (B) Flow cytometric analysis of MDA-MB-231 or MCF7 cells treated with Ru-PIP (25 μM), OLAP (5 μM), or both together, for 24 h. Cells were stained with Annexin V–FITC/PI and analyzed by flow cytometry to determine levels of apoptotic cell death. The percentage of cells in each quadrant is depicted in each scatterplot. Right, quantification of apoptotic cells. Mean +/- SD for three independent experiments. *P < 0.05, **P < 0.01, ***P < 0.001 by ANOVA.

Ru-PIP/olaparib enhances DSB damage and abrogates pChk1 signaling. To examine whether the synergy between Ru-PIP and olaparib was accompanied by increased DNA damage, we assessed the levels of γH2AX (H2AX phosphorylated at Ser139) as an early response to DSB formation.[34] Single-agent treated and untreated cells were used for comparison. In both MDA-MB-231 and MCF7 cells, combination treatment with Ru-PIP and olaparib demonstrated greater levels of γH2AX than single-agent treatments (Figures 4A,B). Single-agent Ru-PIP treatment resulted in comparable γH2AX levels to untreated cells in both cell lines (Figures 4A,B), indicating low DSB damage generated by Ru-PIP. This finding is consistent with our previous study.[29]

Examining Chk1 signaling, a clear increase in pChk1 (Chk1 phosphorylated at Ser345) was observed at early time points in MDA-MB-231 cells treated with Ru-PIP (Figure 4C), consistent with the presence of Ru-PIP stalled replication forks.[29] However, for cells treated with Ru-PIP in the presence of OLAP, much lower pChk1 levels were detected (Figure 4C). These results are consistent with PARPi abrogation of Ru-PIP-activated Chk1 and is also in agreement with the observation that PARPi can prevent replication fork restart and stabilization in a Chk1-dependent manner.[35]

In addition to PARPi facilitated fork collapse, chromatin-bound “trapped” PARP-DNA complexes can generate DSBs upon colliding with active replication forks.[36] To explore the possibility that RuPIP was increasing trapped PARP levels, we examined levels of chromatin-bound PARP1 in MDA-MB-231 cells. While an increase in chromatin-bound (trapped) PARP1 was seen for OLAP-treatment, no evidence of an increase in trapped PARP-DNA complexes was observed in cells treated with the combination (Figure 4D). Together with the previous section, these results are consistent with a mechanism of synergy whereby

PARPi results in collapse of Ru-PIP-stalled replication forks, leading to increased levels of DSB damage before culminating in G2 arrest and ultimately triggering cell death by apoptosis.

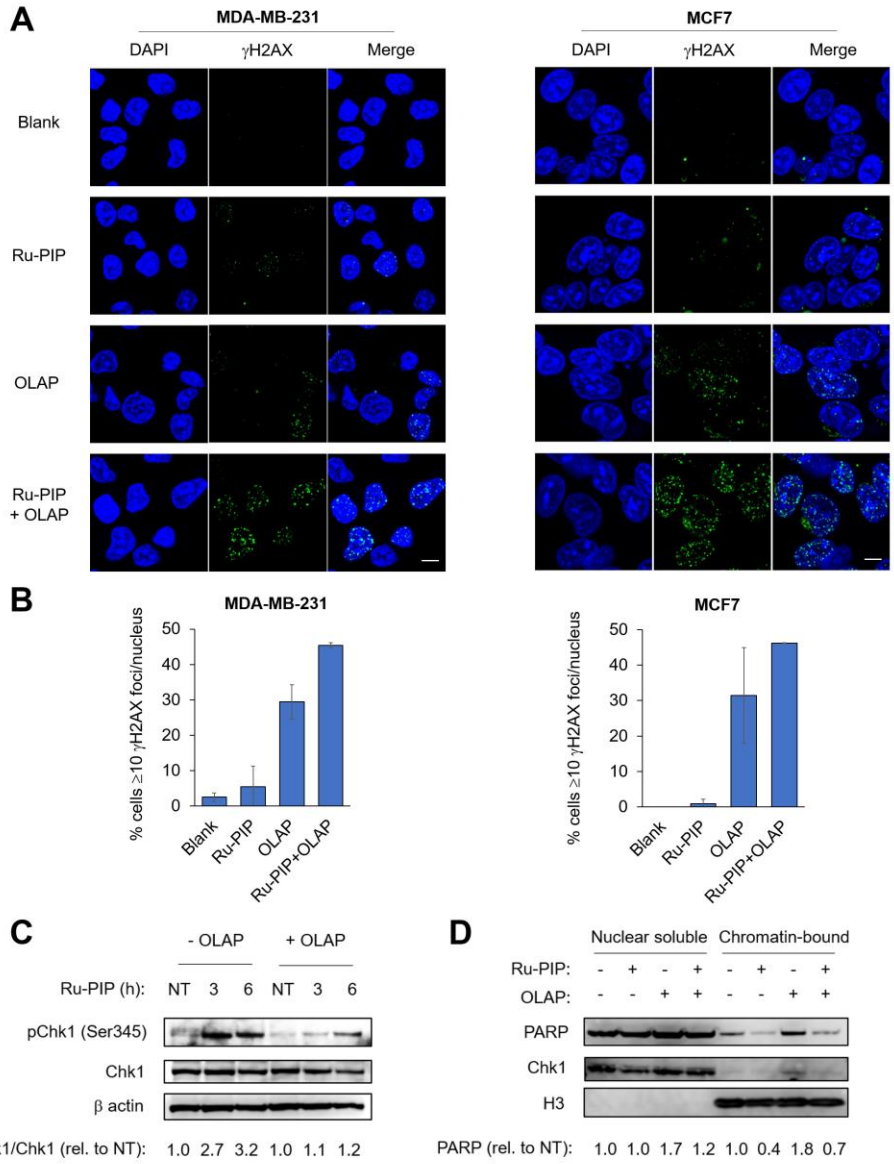

Figure 4. Ru-PIP/olaparib results in enhanced DNA damage versus single-agent treatment. (A) CLSM images of MDA-MB-231 or MCF7 cells treated with Ru-PIP (25 μM), OLAP (5 μM), or the combination of both, for 24 h. Immunofluorescence staining with anti-γH2AX (green) provides visualization of DNA damage (DSB breaks). DNA (DAPI) staining including for reference. (B) Quantification of γH2AX foci for cells treated as in (A). Data expressed as the % of total cell population containing 10 or more foci/nucleus. Mean +/- SD of three (MDA-MB-231) or two (MCF7) independent experiments where a minimum of 400

(MDA-MB-231) or 300 (MCF7) nuclei were counted per condition. (C) Immunoblotting of whole cell extracts of MDA-MB-231 cells treated with Ru-PIP (100 μM, 3 or 6 h) in the absence or presence of OLAP (5 μM) for activated p-Chk1 (Chk1 phosphorylated at Ser345). Levels of total Chk1 protein independent of phosphorylation status are shown. β actin employed as a loading control. (D) Immunoblotting of nuclear soluble and chromatin-bound fractions prepared from MDA-MB-231 cells treated with Ru-PIP (100 μM), OLAP (5 μM), or both (3 h) for PARP1 levels. Chk1 and H3 provide an indication of the successful isolation of nuclear soluble and chromatin-bound fractions respectively. pChk1/Chk1 and PARP1 quantification based on densitometry. NT = not treated.

Ru-PIP/olaparib impedes cell motility. Finally, in addition to its role in DNA repair, sub-lethal doses of olaparib can inhibit migration of cancer cells.[37] Employing a wound "scratch" assay to examine the role of OLAP and Ru-PIP on cell migration, MDA-MB-231 or MCF7 cells treated with the combination of OLAP and Ru-PIP had decreased cell migration compared to a mock-treated control (Figures 5A,B). Single-agent treatment with OLAP had negligible impact on cell migration, while the effects of single-agent Ru-PIP were significantly weaker than the combination. This indicates that the combination of OLAP and Ru-PIP acts to interfere with the invasive potential of breast cancer cells in addition to increasing DNA damage.

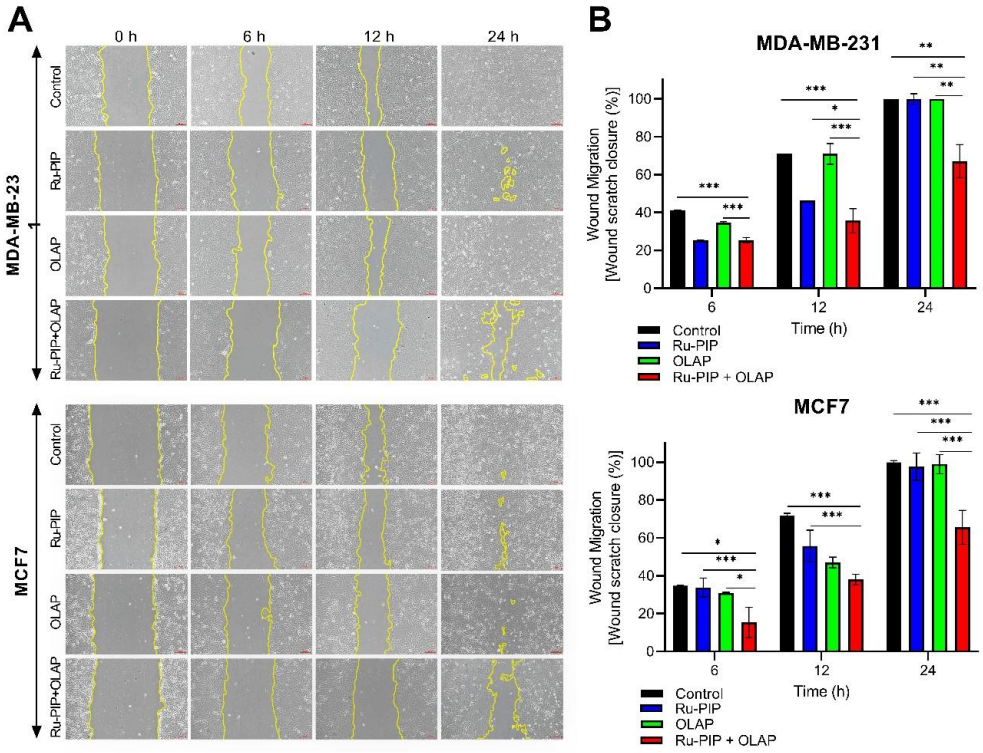

Figure 5. Ru-PIP/olaparib combination impedes cell migration. (A) Representative images of wound-healing assay for MDA-MB-231 or MCF7 cells treated with OLAP (5 μM), Ru-PIP (25 μM), or both. Cells migration was monitored by optical microscopy at the indicated time points. Scale bar, 50 μm. (B) Quantification of percentage of wound closure for cells treated as in (A), as determined by analysis using ImageJ software. Mean +/- S.D. of three independent experiments. *P < 0.05, **P < 0.01, ***P < 0.001 by ANOVA.

Conclusions. Recent years has seen growing interest in the anti-cancer potential of RPCs as single-agents,[38–40] in combination with light for photodynamic therapy, PDT,[41] and also as radiosensitizers for ionizing radiation, IR.[42] However, utilizing RPCs in combination therapy with targeted therapeutics is a relatively unexplored strategy.

These mechanistic studies indicate the observed synergy between the DNA replication inhibitor Ru-PIP and PARP inhibitor olaparib to be the result of enhanced DSB DNA damage, G2/M arrest and apoptosis compared to single-agent conditions. These results are consistent with olaparib acting to facilitate the collapse of Ru-PIP-induced stalled or stabilized replication forks, with the resultant DSB damage then triggering apoptosis. This mechanism of action is similar to a recent study showing PARPi can abrogate the effects of another potent DNA replication inhibitor hydroxyurea (HU) via interfering with PAR

(supplied by PARP) binding Chk1 at stalled replication forks.[35] Considering that pharmacological inhibition studies have indicated that both PARP (this work) and Chk1[29] are required for stabilisation of Ru-PIP-stalled replication forks, it would be interesting to examine PAR recruitment and Chk1 binding to forks stalled by Ru-PIP to explore this in more detail.

Of course, new synergistic combinations identified still need to have cancer-specificity or they risk having low clinical benefit. Although the low impact on normal fibroblasts from the combination treatment isolated by this study is encouraging, fibroblasts can exhibit relatively high resistance to DNA damage and cellular stress.[43] Further work examining a greater range of cell lines, including normal epithelial cells, and *in vivo* studies would be required to fully explore the therapeutic window of this novel combination.

Finally, while Ru-PIP has not been examined *in vivo*, a growing number of RPCs have been examined in this context and no adverse effects have been noted.[44,45] It is particularly noteworthy that Ru-PIP induces replication stress without DSB damage or triggering apoptosis and sensitizes cells to olaparib at doses with minimal single-agent impact on clonogenic survival. This property of Ru-PIP may be advantageous in reducing unfavourable mechanistic overlap with PARPi, particularly as the majority of DNA-targeting agents explored in combination with PARPi to date all act *via* the generation of substantial levels of cytotoxic - and potentially genotoxic - DSB damage. Further studies will examine Ru-PIP - and derivatives - alongside other DDR inhibitors and also examine the potential for applying identified combination therapies in dual drug-delivery applications to further improve cancer-specificity.

Methods

Chemicals and reagents. $[Ru(dppz)_2(PIP)]^{2+}$, Ru-PIP, was synthesized and characterized as reported previously.[29] Olaparib (OLAP) was purchased from Sigma-Aldrich and NU1025 from Enzo Life Sciences. Stock solutions of Ru-PIP (100 mM), NU1025 (10 mM) and OLAP (10 mM) were prepared in 100% dimethyl sulfoxide (DMSO) and further diluted using Dulbecco's modified Eagle's medium (DMEM) or phosphate buffer saline (PBS). Final DMSO concentration employed in cell studies < 0.5%. All negative controls, blanks and "not treated" conditions contained 0.5% DMSO. Antibodies (Company, Lot no.): γH2AX (Millipore, 3108494), PARP1 (Atlas, E115837, a gift from Dr S. Hopkins), β-actin (AbCam,

GR3251792-1), pChk1(Ser345) (Cell Signaling, 02/2019 8), Chk1 (Santa Cruz, 1013), H3 (Invitrogen, 865R2, a gift from Dr G. De Gregoriis).

Cell lines. MCF7 and MDA-MB-231 cell lines were cultured in DMEM supplemented with 10% fetal bovine serum (FBS) and 1% penicillin/streptomycin antibiotic. Normal human dermal fibroblasts (NHDF) were cultured with DMEM supplemented with 5% FBS. All cell lines were maintained at 37 °C under a humidified atmosphere containing 5% CO_2 and routinely sub-cultured with Trypsin.

Drug interaction analysis. Dose-effect curves for single agents and their combinations were generated from MTT assay data and the combination index (CI) values calculated using CalcuSyn and Compusyn software (Biosoft, Cambridge, UK) as established by Chou and Talalay.[33] CI < 0.8 indicates synergism, CI = 0.8-1 indicates additive and CI > 1 indicates antagonism. Microsoft Excel was used to generate a 3-color scale based on CI values obtained, where synergism is represented by green color, additive by yellow and antagonism by red. The color of each CI value were interpolated in-between these constraints accordingly.

Clonogenic survival assay. Cells were seeded at 1 x 10^5 cells/well in 6-well plates and allowed to adhere for 24 h. Cells were treated with the stated single-agent or combination for the required time of incubation (24 and 48 h). After treatment, solutions were removed and cells were trypsinized, re-seeded in a new 6-well plate at a density of 1x10^3 cells/well, and cultured in compound-free medium. Cells were incubated for 7-10 days to allow colony formation. Cells were then fixed with fixation solution [methanol:glacial acetic acid, 3:1 (v:v)] for 15 mins and stained with 0.4 % methylene blue for 20 mins. The staining solution was washed with water and images were photographed with a digital camera. Individual colonies were counted using Image J software, and the survival fraction was determined (normalized to controls). Experiments were repeated three independent times.

Cell cycle analysis. Cells were seeded at 1 x 10^5 cells/well in 6-well plates and allowed to adhere for 24 h. Cells were then treated with with Ru-PIP (25 μM), NU1025 (25 μM), and OLAP (5 μM) alone and in combination for 24 h. After treatment, cells were trypsinized and washed with PBS twice. Cells were then fixed with 70% ice-cold ethanol for at least

overnight at 4°C. Following fixation, fixed cells were centrifuged at 13,000 rpm for 5 mins and the resulting pellet were washed with PBS twice. The samples were then resuspended in 500 μl PBS and treated with 50 μl RNase A solution (1 mg/ml). After 15 mins of incubation, the samples were stained with 200 μl of 50 μg/ml propidium iodide (PI) solution at RT. Samples were acquired and analyzed with NovoCyte flow cytometer (ACEA Biosciences, San Diego, CA, USA) and NovoExpress software. For each sample, a minimum of 10,000 cells were counted.

Apoptosis Annexin V/FITC assay. Cells were seeded at a density of 1 x 10^5 cells/well in a 6-well plate and allowed to adhere for 24 h. Cells were treated with Ru-PIP (25 μM) and/or OLAP (5 μM) for 24 h. After treatment, cells were trypsinized, washed with PBS and followed by the addition of 500 μl of 1x binding buffer and 5 μl Annexin V-FITC (Invitrogen). The cell-containing mixture was then incubated for 20 mins at room temperature (RT). PI (5 μl) was added prior to flow cytometric analysis using NovoCyte flow cytometer, and results were analyzed using NovoExpress software. For each sample, a minimum of 10,000 cells were counted.

Immunoblotting and immunofluorescence. Whole cell lysates of treated samples were prepared as described previously.[30] For isolation of nuclear soluble and chromatin-bound subcellular fractions, treated cells were processed with the Subcellular Protein Fractionation kit for Cultured Cells (Thermo) according to the manufacturer's instructions. Isolated nuclear soluble and chromatin-bound fractions for each treatment group were obtained and protein concentration quantified by BCA assay. Aliquots of cell lysates or fractions were prepared in standard Laemmli buffer, heated at 95 °C for 5 mins and resolved by NuPAGE® 4–12% pre-cast Bis-Tris gels and LDS-PAGE. Gels were transferred onto nitrocellulose membrane and probed with primary antibodies in 5% BSA (bovine serum albumin) solutions. Reactions were visualized with a suitable secondary antibody conjugated with horseradish peroxidase (1/5000 dilution, Thermo). WesternSurePREMIUM (Li-Cor) chemiluminescent substrates with digital analysis (LiCor C-Digit Blot Scanner) were used to visualize protein expression. Densitometry data was acquired using Image Studio™ Software supplied with the C-Digit Scanner. Immunofluorescence (γH2AX foci) was performed as described previously.[30]

Scratch "wound" assay. Cells were seeded at $5x10^5$ cells/well in 6-well plates and left in the incubator until a confluent monolayer of cells formed. By using a sterile 200 μl pipette tip, a straight scratch was made in each well and was washed with PBS twice. Cells were then treated with Ru-PIP (25 μM) and/or OLAP (5 μM). The migration of the cells in the wound scratch area was analyzed and photographed at 0 h, 6 h, 12 h, and 24 h. Images were photographed at 10x magnification using a microscope attached to a digital camera and the images captured were analyzed using ImageJ software. The percentage of wound scratch closure was determined by measuring the reduction in the area of the wound at each time point and compared to 0 h (100%).

Statistical analysis. Statistical analysis of the data and the representation of figures were done using GraphPad Prism software. By using GraphPad Prism software, statistical analysis of the data was analyzed by using one-way analysis of variance (ANOVA), and the differences between the groups studied were considered significant when *P* values generated were less than 0.05.

Supplementary Methods. MTT assay and Trypan Blue exclusion assay methods are in the Supporting Information.

Associated content

Supporting Information Available: This material is available free of charge via the Internet. Supplementary Methods. Supplementary Figures 1-4. Supplementary Table 1.

Author Information

Corresponding authors

*E-mail: m.r.gill@swansea.ac.uk

*E-mail: haslina_ahmad@upm.edu.my

ORCID

Katherine A. Vallis: 0000-0003-4672-5683

Martin R. Gill: 0000-0002-1371-5676

Notes

The authors declare no competing financial interest.

Acknowledgements

This study was supported by the Ministry of Education Malaysia through FRGS/1/2017/STG01/UPM/02/6 (01-01-17-1913FR) for the "In Vitro Evaluation of Novel Mesoporous Silica Nanovehicles for the delivery of Ruthenium(II) Anticancer Drug". M. R. G. and K. A. V. acknowledge financial support from Cancer Research UK (C5255/A15935).

References

(1) Schneider, B. P., Winer, E. P., Foulkes, W. D., Garber, J., Perou, C. M., Richardson, A., Sledge, G. W., and Carey, L. A. (2008) Triple-negative breast cancer: Risk factors to potential targets. *Clin. Cancer Res. 14*, 8010–8018.

(2) Foulkes, W. D., Smith, I. E., and Reis-Filho, J. S. (2010) Triple-negative breast cancer. *N. Engl. J. Med. 363*, 1938–1948.

(3) Carey, L., Winer, E., Viale, G., Cameron, D., and Gianni, L. (2010) Triple-negative breast cancer: disease entity or title of convenience? *Nat. Rev. Clin. Oncol. 7*, 683–692.

(4) Liu, J. C., Granieri, L., Shrestha, M., Wang, D.-Y., Vorobieva, I., Rubie, E. A., Jones, R., Ju, Y., Pellecchia, G., Jiang, Z., Palmerini, C. A., Ben-David, Y., Egan, S. E., Woodgett, J. R., Bader, G. D., Datti, A., and Zacksenhaus, E. (2018) Identification of CDC25 as a common therapeutic target for triple-negative breast cancer. *Cell Rep. 23*, 112–126.

(5) Yang, Y.-G., Cortes, U., Patnaik, S., Jasin, M., and Wang, Z.-Q. (2004) Ablation of PARP-1 does not interfere with the repair of DNA double-strand breaks, but compromises the reactivation of stalled replication forks. *Oncogene 23*, 3872–3882.

(6) Bryant, H. E., Schultz, N., Thomas, H. D., Parker, K. M., Flower, D., Lopez, E., Kyle, S., Meuth, M., Curtin, N. J., and Helleday, T. (2005) Specific killing of BRCA2-deficient tumours with inhibitors of poly(ADP-ribose) polymerase. *Nature 434*, 913–917.

(7) Farmer, H., McCabe, N., Lord, C. J., Tutt, A. N. J., Johnson, D. A., Richardson, T. B., Santarosa, M., Dillon, K. J., Hickson, I., Knights, C., Martin, N. M. B., Jackson, S. P., Smith, G. C. M., and Ashworth, A. (2005) Targeting the DNA repair defect in BRCA mutant cells as a therapeutic strategy. *Nature 434*, 917–921.

(8) Mateo, J., Lord, C. J., Serra, V., Tutt, A., Balmaña, J., Castroviejo-Bermejo, M., Cruz, C., Oaknin, A., Kaye, S. B., and de Bono, J. S. (2019) A decade of clinical development of PARP inhibitors in perspective. *Ann. Oncol. 30*, 1437–1447.

(9) Robson, M., Im, S.-A., Senkus, E., Xu, B., Domchek, S. M., Masuda, N., Delaloge, S., Li,

W., Tung, N., Armstrong, A., Wu, W., Goessl, C., Runswick, S., and Conte, P. (2017) Olaparib for metastatic breast cancer in patients with a germline BRCA mutation. *N. Engl. J. Med. 377*, 523–533.
(10) Yap, T. A., Plummer, R., Azad, N. S., and Helleday, T. (2019) The DNA damaging revolution: PARP inhibitors and beyond. *Am. Soc. Clin. Oncol. Edu. Book.* 185–195.
(11) Narod, S. A. (2010) BRCA mutations in the management of breast cancer: the state of the art. *Nat. Rev. Clin. Oncol. 7*, 702–707.
(12) Pilie, P., Gay, C. M., Byers, L. A., O'Connor, M. J., and Yap, T. A. (2019) PARP inhibitors: Extending benefit beyond BRCA mutant cancers. *Clin. Cancer Res. 25*, 3759–3771.
(13) Evers, B., Drost, R., Schut, E., de Bruin, M., van der Burg, E., Derksen, P. W. B., Holstege, H., Liu, X., van Drunen, E., Beverloo, H. B., Smith, G. C. M., Martin, N. M. B., Lau, A., O'Connor, M. J., and Jonkers, J. (2008) Selective inhibition of BRCA2-deficient mammary tumor cell growth by AZD2281 and cisplatin. *Clin. Cancer Res. 14*, 3916–3925.
(14) Shen, Y. T., Evans, J. C., Zafarana, G., Allen, C., and Piquette-Miller, M. (2018) BRCA status does not predict synergism of a carboplatin and olaparib combination in high-grade serous ovarian cancer cell lines. *Mol. Pharmaceutics 15*, 2742–2753.
(15) Eetezadi, S., Evans, J. C., Shen, Y.-T., De Souza, R., Piquette-Miller, M., and Allen, C. (2018) Ratio-dependent synergism of a doxorubicin and olaparib combination in 2D and spheroid models of ovarian cancer. *Mol. Pharmaceutics 15*, 472–485.
(16) Oza, A. M., Cibula, D., Benzaquen, A. O., Poole, C., Mathijssen, R. H. J., Sonke, G. S., Colombo, N., Špaček, J., Vuylsteke, P., Hirte, H., Mahner, S., Plante, M., Schmalfeldt, B., Mackay, H., Rowbottom, J., Lowe, E. S., Dougherty, B., Barrett, J. C., and Friedlander, M. (2015) Olaparib combined with chemotherapy for recurrent platinum-sensitive ovarian cancer: a randomised phase 2 trial. *Lancet Oncol. 16*, 87–97.
(17) Balmaña, J., Tung, N. M., Isakoff, S. J., Graña, B., Ryan, P. D., Saura, C., Lowe, E. S., Frewer, P., Winer, E., Baselga, J., and Garber, J. E. (2014) Phase I trial of olaparib in combination with cisplatin for the treatment of patients with advanced breast, ovarian and other solid tumors. *Ann. Oncol. 25*, 1656–1663.
(18) González-Martín, A., Pothuri, B., Vergote, I., DePont Christensen, R., Graybill, W., Mirza, M. R., McCormick, C., Lorusso, D., Hoskins, P., Freyer, G., Baumann, K., Jardon, K., Redondo, A., Moore, R. G., Vulsteke, C., O'Cearbhaill, R. E., Lund, B., Backes, F., Barretina-Ginesta, P., Haggerty, A. F., Rubio-Pérez, M. J., Shahin, M. S., Mangili, G., Bradley, W. H., Bruchim, I., Sun, K., Malinowska, I. A., Li, Y., Gupta, D., and Monk, B. J.

(2019) Niraparib in patients with newly diagnosed advanced ovarian cancer. *N. Engl. J. Med. 381*, 2391-2402.
(19) LaFargue, C. J., Dal Molin, G. Z., Sood, A. K., and Coleman, R. L. (2019) Exploring and comparing adverse events between PARP inhibitors. *Lancet Oncol. 20*, e15–e28.
(20) Lallo, A., Frese, K. K., Morrow, C. J., Sloane, R., Gulati, S., Schenk, M. W., Trapani, F., Simms, N., Galvin, M., Brown, S., Hodgkinson, C. L., Priest, L., Hughes, A., Lai, Z., Cadogan, E., Khandelwal, G., Simpson, K. L., Miller, C., Blackhall, F., O'Connor, M. J., and Dive, C. (2018) The combination of the PARP inhibitor olaparib and the WEE1 inhibitor AZD1775 as a new therapeutic option for small cell lung cancer. *Clin. Cancer Res. 24*, 5153–5164.
(21) Yazinski, S. A., Comaills, V., Buisson, R., Genois, M.-M., Nguyen, H. D., Ho, C. K., Todorova Kwan, T., Morris, R., Lauffer, S., Nussenzweig, A., Ramaswamy, S., Benes, C. H., Haber, D. A., Maheswaran, S., Birrer, M. J., and Zou, L. (2017) ATR inhibition disrupts rewired homologous recombination and fork protection pathways in PARP inhibitor-resistant BRCA-deficient cancer cells. *Genes Dev. 31*, 318–332.
(22) Muvarak, N. E., Chowdhury, K., Xia, L., Robert, C., Choi, E. Y., Cai, Y., Bellani, M., Zou, Y., Singh, Z. N., Duong, V. H., Rutherford, T., Nagaria, P., Bentzen, S. M., Seidman, M. M., Baer, M. R., Lapidus, R. G., Baylin, S. B., and Rassool, F. V. (2016) Enhancing the cytotoxic effects of PARP inhibitors with DNA demethylating agents; a potential therapy for cancer. *Cancer Cell 30*, 637–650.
(23) Matulonis, U. A., and Monk, B. J. (2017) PARP inhibitor and chemotherapy combination trials for the treatment of advanced malignancies: does a development pathway forward exist? *Ann. Oncol. 28*, 443–447.
(24) Falchi, F., Giacomini, E., Masini, T., Boutard, N., Di Ianni, L., Manerba, M., Farabegoli, F., Rossini, L., Robertson, J., Minucci, S., Pallavicini, I., Di Stefano, G., Roberti, M., Pellicciari, R., and Cavalli, A. (2017) Synthetic lethality triggered by combining olaparib with BRCA2–Rad51 disruptors. *ACS Chem. Biol. 12*, 2491–2497.
(25) Bryant, H. E., Petermann, E., Schultz, N., Jemth, A.-S., Loseva, O., Issaeva, N., Johansson, F., Fernandez, S., McGlynn, P., and Helleday, T. (2009) PARP is activated at stalled forks to mediate Mre11-dependent replication restart and recombination. *EMBO J. 28*, 2601–2615.
(26) Ronson, G. E., Piberger, A. L., Higgs, M. R., Olsen, A. L., Stewart, G. S., McHugh, P. J., Petermann, E., and Lakin, N. D. (2018) PARP1 and PARP2 stabilise replication forks at base excision repair intermediates through Fbh1-dependent Rad51 regulation. *Nat. Commun.*

9, 746.
(27) Liao, H., Ji, F., Helleday, T., and Ying, S. (2018) Mechanisms for stalled replication fork stabilization: new targets for synthetic lethality strategies in cancer treatments. *EMBO Rep. 19*, e46263.
(28) Zeglis, B. M., Pierre, V. C., and Barton, J. K. (2007) Metallo-intercalators and metallo-insertors. *Chem. Commun.* 4565–4579.
(29) Gill, M. R., Harun, S. N., Halder, S., Boghozian, R. A., Ramadan, K., Ahmad, H., and Vallis, K. A. (2016) A ruthenium polypyridyl intercalator stalls DNA replication forks, radiosensitizes human cancer cells and is enhanced by Chk1 inhibition. *Sci. Rep. 6*, 31973.
(30) Gill, M. R., Jarman, P. J., Halder, S., Walker, M. G., Saeed, H. K., Thomas, J. A., Smythe, C., Ramadan, K., and Vallis, K. A. (2018) A three-in-one-bullet for oesophageal cancer: Replication fork collapse, spindle attachment failure and enhanced radiosensitivity generated by a ruthenium(II) metallo-intercalator. *Chem. Sci. 9*, 841–849.
(31) Bowman, K. J., Newell, D. R., Calvert, A. H., and Curtin, N. J. (2001) Differential effects of the poly (ADP-ribose) polymerase (PARP) inhibitor NU1025 on topoisomerase I and II inhibitor cytotoxicity in L1210 cells in vitro. *Br. J. Cancer 84*, 106–112.
(32) Elstrodt, F., Hollestelle, A., Nagel, J. H. A., Gorin, M., Wasielewski, M., van den Ouweland, A., Merajver, S. D., Ethier, S. P., and Schutte, M. (2006) BRCA1 mutation analysis of 41 human breast cancer cell lines reveals three new deleterious mutants. *Cancer Res. 66*, 41–45.
(33) Chou, T.-C., and Talalay, P. (1984) Quantitative analysis of dose-effect relationships: the combined effects of multiple drugs or enzyme inhibitors. *Adv. Enzyme Regul. 22*, 27–55.
(34) Rogakou, E. P., Pilch, D. R., Orr, A. H., Ivanova, V. S., and Bonner, W. M. (1998) DNA double-stranded breaks induce histone H2AX phosphorylation on serine 139. *J. Biol. Chem. 273*, 5858–5868.
(35) Min, W., Bruhn, C., Grigaravicius, P., Zhou, Z.-W., Li, F., Krüger, A., Siddeek, B., Greulich, K.-O., Popp, O., Meisezahl, C., Calkhoven, C. F., Bürkle, A., Xu, X., and Wang, Z.-Q. (2013) Poly(ADP-ribose) binding to Chk1 at stalled replication forks is required for S-phase checkpoint activation. *Nat. Commun. 4*, 2993.
(36) Murai, J., Huang, S. N., Das, B. B., Renaud, A., Zhang, Y., Doroshow, J. H., Ji, J., Takeda, S., and Pommier, Y. (2012) Trapping of PARP1 and PARP2 by clinical PARP inhibitors. *Cancer Res. 72*, 5588–5599.
(37) Prasad, C. B., Prasad, S. B., Yadav, S. S., Pandey, L. K., Singh, S., Pradhan, S., and Narayan, G. (2017) Olaparib modulates DNA repair efficiency, sensitizes cervical cancer

cells to cisplatin and exhibits anti-metastatic property. *Sci. Rep. 7*, 12876.
(38) Notaro, A., and Gasser, G. (2017) Monomeric and dimeric coordinatively saturated and substitutionally inert Ru(ii) polypyridyl complexes as anticancer drug candidates. *Chem. Soc. Rev. 46*, 7317–7337.
(39) Poynton, F. E., Bright, S. A., Blasco, S., Williams, D. C., Kelly, J. M., and Gunnlaugsson, T. (2017) The development of ruthenium(ii) polypyridyl complexes and conjugates for in vitro cellular and in vivo applications. *Chem. Soc. Rev. 46*, 7706–7756.
(40) Zeng, L., Gupta, P., Chen, Y., Wang, E., Ji, L., Chao, H., and Chen, Z.-S. (2017) The development of anticancer ruthenium(ii) complexes: from single molecule compounds to nanomaterials. *Chem. Soc. Rev. 46*, 5771–5804.
(41) Mari, C., Pierroz, V., Ferrari, S., and Gasser, G. (2015) Combination of Ru(ii) complexes and light: new frontiers in cancer therapy. *Chem. Sci. 6*, 2660–2686.
(42) Gill, M. R., and Vallis, K. A. (2019) Transition metal compounds as cancer radiosensitizers. *Chem. Soc. Rev. 48*, 540–557.
(43) Mapuskar, K. A., Flippo, K. H., Schoenfeld, J. D., Riley, D. P., Strack, S., Hejleh, T. A., Furqan, M., Monga, V., Domann, F. E., Buatti, J. M., Goswami, P. C., Spitz, D. R., and Allen, B. G. (2017) Mitochondrial superoxide increases age-associated susceptibility of human dermal fibroblasts to radiation and chemotherapy. *Cancer Res. 77*, 5054–5067.
(44) Yadav, A., Janaratne, T., Krishnan, A., Singhal, S. S., Yadav, S., Dayoub, A. S., Hawkins, D. L., Awasthi, S., and MacDonnell, F. M. (2013) Regression of lung cancer by hypoxia-sensitizing ruthenium polypyridyl complexes. *Mol. Cancer Ther. 12*, 643–653.
(45) Zhou, Y., Xu, Y., Lu, L., Ni, J., Nie, J., Cao, J., Jiao, Y., and Zhang, Q. (2019) Luminescent ruthenium(II) polypyridyl complexes acted as radiosensitizer for pancreatic cancer by enhancing radiation-induced DNA damage. *Theranostics 9*, 6665–6675.